Fermi National Accelerator Laboratory

FERMILAB-PUB-95/160-T
UCD-95-17
UCLA/95/TEP/24
AMES-HET-95-01
June 1995

Top-Quark Decay Via Flavor-Changing Neutral Currents at Hadron Colliders

T. Han[a], R.D. Peccei[b], and X. Zhang[c]

[a] *Department of Physics, University of California, Davis, CA 95616, USA*

[b] *Department of Physics, University of California, Los Angeles, CA 90024, USA*

[c] *Department of Physics and Astronomy, Iowa State University, Ames, IA 50011, USA*

and

Fermi National Accelerator Laboratory, P. O. Box 500, Batavia, IL 60510, USA

Abstract

We study low energy experimental constraints on an anomalous top-quark coupling associated with the flavor-changing neutral current vertex $Z\bar{t}c$. In view of these constraints, we discuss the experimental observability of the induced rare decay mode $t \to Zc$, both at the Fermilab Tevatron (with the Main Injector or a luminosity-upgrade) and at the LHC.

I. INTRODUCTION

The existence of the top quark has been established recently at the Fermilab Tevatron by the CDF and D0 collaborations [1] with a measured mass near 175 GeV. Because the top quark is heavier than all other observed fermions and gauge bosons and has a mass of the

Operated by Universities Research Association Inc. under contract with the United States Department of Energy

order of the Fermi scale, it couples to the electroweak symmetry breaking sector strongly. In its simplest incarnation, the symmetry breaking sector of the Standard Model (SM) results from the presence of a complex fundamental Higgs scalar in the theory. However, there are theoretical arguments of "triviality" [2] and "naturalness" [3] which mitigate against having such a simple scalar sector. One therefore believes that the Higgs sector of the Standard Model is just an effective theory, and expects that new physics phenomena will manifest themselves significantly through effective interactions of the top quark [4].

If anomalous top-quark couplings beyond the SM were to exist, they would affect top-quark production and decay processes at hadron and e^+e^- colliders [5,6]. Furthermore, such couplings would also affect some quantities measured with high precision, such as the partial width of $Z \to b\bar{b}$. The experimentally observed value at LEP-I for the partial width ratio $R_b = \Gamma(Z \to b\bar{b})/\Gamma(Z \to \text{Hadrons})$ is somewhat higher than the Standard Model expectation [7]. This could be the result of a statistical fluctuation, or it could also be an indication of new physics.

In this paper, we will study the experimental constraints on an anomalous top-quark coupling $Z\bar{t}c$ [8] and discuss in detail the experimental observability of the induced rare decay mode $t \to Zc$ [9], both at the Fermilab Tevatron and the LHC. There are two major motivations for such a study. First of all, it is argued [8] that, in a dynamical electroweak symmetry breaking scheme, the coupling parameters, κ_{ij}, which typify the anomalous couplings of the Z boson to fermions i and j, may behave like,

$$\kappa_{ij} \sim O(\frac{\sqrt{m_i m_j}}{v}), \tag{1}$$

with m_i being the mass of the fermion i, and v the vacuum expectation value $v \simeq 250$ GeV. This estimate is consistent with the bounds on the κ_{ij} for the light quarks [8] and may give significant effects for the heavy top-quark sector. Representative models in which the above enhancement may be realized include those with new dynamical interactions of the top quarks [10], with multi-Higgs doublets [11,12], and with new exotic fermions [13]. Secondly, the decay $t \to Zc$ is rather unique. It has a very distinct experimental signature, especially

if we look for the clean final state from $Z \to l^+l^-$ at hadron colliders. Moreover, what makes this study very important is that the expected value of the branching fraction BR($t \to Zc$) in the SM is extremely small, being of an order of 10^{-12} [11]. Thus, the observation of such a top-quark decay mode would signal the existence of new physics. As we shall see, the Fermilab Tevatron with an integrated luminosity of 10 fb^{-1} and the LHC with 100 fb^{-1} will have good potential to explore this anomalous $Z\bar{t}c$ vertex.

This paper is organized as follows. In Section II, we examine the current low energy constraints on the anomalous $Z\bar{t}c$ coupling. In Section III, we study the possibility of testing this anomalous coupling at the Fermilab Tevatron and the LHC. Finally, in Section IV, we summarize our results. The helicity amplitudes for $t \to Zc$ decay are presented in an appendix.

II. LOW ENERGY CONSTRAINTS ON THE ANOMALOUS $Z\bar{T}C$ COUPLING

Following Ref. [4], we introduce an effective lagrangian involving the anomalous top-quark couplings,

$$\mathcal{L}^{eff} = \mathcal{L}^{SM} + \Delta\mathcal{L}^{eff} \tag{2}$$

where $\mathcal{L}^{SM}$ is the Standard Model lagrangian and $\Delta\mathcal{L}^{eff}$ includes all of the anomalous top-quark couplings. For the purpose of this paper, we consider only the anomalous couplings associated with the $Z\bar{t}c$ vertex, and only the operators of lowest dimension that contribute. Then

$$\Delta\mathcal{L}^{eff} = -\frac{g}{2\cos\theta_W}\left[\kappa_L Z^\mu \bar{t}\gamma_\mu(\frac{1-\gamma_5}{2})c + \kappa_R Z^\mu \bar{t}\gamma_\mu(\frac{1+\gamma_5}{2})c\right] + h.c.\,, \tag{3}$$

where g is the coupling constant of $SU(2)_L$, θ_W is the Weinberg mixing angle and $\kappa_{L(R)}$ are free parameters determining the strength of these anomalous couplings. Assuming CP-invariance, $\kappa_{L(R)}$ are real.

The lagrangian $\Delta\mathcal{L}^{eff}$ of Eq. (3) is written in the unitary gauge with a non-linear realization of $SU(2)_L \times U(1)_Y$. The details of the fermion transformation rule and the

procedure for constructing the invariant effective lagrangian under the nonlinear $SU(2)_L \times U(1)_Y$ group has been given in [4], and will not be repeated here. However, it is important to emphasize that because $SU(2)_L \times U(1)_Y$ is spontaneously broken down to $U(1)_{em}$, the anomalous $Z\bar{t}c$ couplings, as well as those of $Z\bar{t}t$ and $W\bar{t}b$, can exist in dimension four, in contrast to the anomalous couplings of a photon (or a gluon) to $\bar{t}c$ or $\bar{t}t$ which require the presence of the gauge field strengths $F_{\mu\nu}$ ($G^a_{\mu\nu}$).

A. Constraints on κ_L

The anomalous coupling κ_L in Eq. (3) is constrained by experimental upper bounds on the induced flavor-changing neutral couplings of the light fermions. Integrating the heavy top quark out of $\mathcal{L}^{eff}$ generates an effective interaction of the form

$$\tilde{\mathcal{L}} = \frac{g}{\cos\theta_W} a_{ij} \bar{f}_i \gamma^\mu (\frac{1-\gamma_5}{2}) f_j Z_\mu + h.c. \tag{4}$$

where $f_i = b,\ s,\ d$. Evaluating the one-loop diagram for the vertex correction gives

$$a_{ij} = \frac{\kappa_L}{16\pi^2} \frac{m_t^2}{v^2} \left(V_{ti} V_{cj}^* + V_{tj} V_{ci}^*\right) \ln\frac{\Lambda^2}{m_t^2}, \tag{5}$$

where V_{ij} are the elements of the Cabbibo-Kobayashi-Maskawa matrix and Λ is a cutoff for the effective lagrangian. The effective lagrangian in Eqs. (2) and (3) is not renormalizable in the common sense. In our calculation we use dimensional regularization to regularize the divergent loop integration [8]. Practically, we have also focused only on certain "log-enhanced" terms by replacing $1/\epsilon$ by $\ln(\Lambda^2/m_t^2)$ in the final results. Note that although we perform the calculation in the unitary gauge, it can be shown easily that our results for a_{ij} are gauge-independent.

To get a more stringent upper limit on κ_L, we take the maximal values of the V_{ti} and V_{cj} matrix elements from the particle data book [14]. Further we use the upper bounds on a_{ij} derived in Ref. [15] by studying several flavor-changing processes, such as $K_L \to \bar{\mu}\mu$, the $K_L - K_S$ mass difference, $B^0 - \bar{B}^0$ mixing and $B \not\to l^+ l^- X$, reproduced below

$$a_{sd} < 2 \times 10^{-5}; \;\; a_{bd} < 4 \times 10^{-4}; \;\; a_{bs} < 2 \times 10^{-3}.$$

Taking Λ =1 TeV and m_t = 175 GeV, this gives an upper limit

$$\kappa_L < 0.05. \tag{6}$$

This upper bound on κ_L is more stringent than what can be derived from the experimental measurement of the partial width of $Z \to \bar{b}b$ at LEP-I. That is, κ_L would have to be bigger than 0.05 to account for the discrepancy with the SM expectations. The bound obtained above using Eq. (5) depends on Λ, so it only gives an order of magnitude upper limit estimate on κ_L. Obviously these bounds are not a substitute for direct measurements. However, perhaps surprisingly these experimental bounds are close to the theoretical values inferred for the anomalous $Z\bar{t}c$ couplings using Eq. (1).

B. Constraints on κ_R

For massless external fermions, κ_R will not contribute to a_{ij}. However, both κ_R and κ_L contribute to the oblique corrections measured experimentaly at LEP-I and the SLC. Consider the vacuum polarization tensor [8] $\Pi^{\mu\nu}_{ZZ}(q^2)$. The presence of $\kappa_{L(R)}$ will generate a term like

$$g^{\mu\nu}(-i)\frac{3}{16\pi^2}\frac{g^2}{4\cos\theta_W^2}(\kappa_L^2+\kappa_R^2)(\frac{4}{3}q^2-2m_t^2)\ln\frac{\Lambda^2}{m_t^2}. \tag{7}$$

Such a contribution will affect quantities like the ρ and S parameters. The strongest constraint on κ_R comes from the ρ parameter. Using the recent determination of the change of ρ from unity, $\Delta\rho = 0.0004 \pm 0.0022 \pm 0.002$ [14], one obtains a 2σ-limit,

$$\kappa_{tc}^2 \equiv \kappa_L^2 + \kappa_R^2 \leq 0.084. \tag{8}$$

In view of the bound on κ_L of Eq. (6), this gives a limit $\kappa_R \leq 0.29$. The S parameter does not improve on this upper bound for κ_R. For $\kappa_L \sim 0.05$, $\kappa_R \sim 0.29$, one finds that

$S^{new} \sim -0.1$. This correction is safely within the present experimental limit [14] for $S^{new} = -0.42 \pm 0.36^{-0.08}_{+0.17}$.

We conclude this section by summarizing the current upper bounds on κ_L and κ_R:

$$\kappa_L \leq 0.05; \quad \kappa_R \leq 0.29; \quad \text{or} \quad \kappa_{tc} \leq 0.29. \tag{9}$$

III. TOP-QUARK DECAY TO Z-CHARM AT HADRON COLLIDERS

At the Fermilab Tevatron, the cross section for $t\bar{t}$ production is about 5 pb with $\sqrt{s} = 2$ TeV [16]. It is conceivable that a comprehensive study of top-quark physics will be carried out with the Main Injector (an integrated luminosity about 1 fb^{-1}/yr expected), or an upgraded Tevatron (about 10 fb^{-1}/yr). The top quarks will be more copiously produced at the LHC due to a much larger center of mass energy (14 TeV) and higher luminosity (100 fb^{-1}/yr). It is therefore interesting to study the feasibility of testing the anomalous $Z\bar{t}c$ couplings at these hadron colliders.

A. Top-Quark Decay to Zc

To a good approximation, we can safely ignore the masses of c and b quarks compared to m_t. The decay $t \to Zc$ [9] is similar to that of $t \to Wb$, up to the new couplings and a kinematical correction factor. We can thus calculate the branching fraction for $t \to Zc$ by the following simple formula,

$$BR(t \to Zc) \equiv \frac{\Gamma(t \to Zc)}{\Gamma(t \to Wb)} = \frac{\kappa_{tc}^2}{2} \frac{(m_t^2 - M_Z^2)^2}{(m_t^2 - M_W^2)^2} \frac{(m_t^2 + 2M_Z^2)}{(m_t^2 + 2M_W^2)} \simeq 0.5\kappa_{tc}^2. \tag{10}$$

Figure 1 shows this branching fraction plotted versus $\kappa_{tc} = \sqrt{\kappa_L^2 + \kappa_R^2}$ for m_t =160 and 200 GeV. From the figure we see that the resulting branching fraction is rather insensitive to the precise value of the top-quark mass, so we will take m_t =175 GeV throughout the paper. The $t \to Zc$ branching fraction is of order 0.1% for $\kappa_{tc} \sim 0.05$, and of order 1% for $\kappa_{tc} \sim 0.15$.

The helicity amplitudes for the decay $t \to Zc$ are presented in an appendix. One sees that a heavy top-quark decays more significantly to a longitudinally polarized vector boson. Keeping only these terms, the charm-jet angular distribution from a left-handed (right-handed) top-quark decay goes approximately like

$$\frac{d\Gamma_{L(R)}}{d\cos\theta} \sim \frac{m_t^2}{M_Z^2}\,[\kappa_{L(R)}^2 \cos^2\frac{\theta}{2} + \kappa_{R(L)}^2 \sin^2\frac{\theta}{2}]. \tag{11}$$

Here the top-quark polarization and the charm-jet polar angle θ are defined in the top-quark rest frame with respect to the direction of its motion. One could imagine trying to explore the underlying couplings $\kappa_{L(R)}$ by studying the angular distributions of the decay products from polarized top quarks. Unfortunately, the dominant mechanisms for top-quark production at hadron colliders via $q\bar{q}$ and gg annihilation give little polarization. This makes the detailed study of these angular distributions impossible. To pursue this further, one will have to study other production mechanisms with larger top-quark polarization, such as single-top production [17,18]. In what follows, we will ignore top-quark polarization effects altogether.

B. Searching for a $t \to Zc$ Signal at Hadron Colliders

To obtain the signal event rates, we calculate the top-quark production via $q\bar{q}, gg \to t\bar{t}$ with lowest order matrix elements, but normalize the total cross sections to values which include higher order corrections [16]. We have used the recent parton distribution functions MRS Set-A [19]. Due to the enormous QCD backgrounds at hadron colliders, it is very difficulty, if not impossible, to search for the signal via the hadronic W, Z decay channels, such as $t\bar{t} \to W^\pm bZc \to W^\pm + 4$-jets [20] or $Z + 4$-jets [21]. For our analysis, we therefore will mainly concentrate on the pure leptonic decays of W and Z, namely: $t \to Wb \to l^\pm \nu b$ and $t \to Zc \to l^+l^-c$, calculated with exact decay matrix elements for on-shell W, Z. We have ignored the spin correlations for the decaying top quarks, as discussed above, due to rather insignificant top-quark polarization [22] for the production mechanisms considered here.

Figure 2 presents the calculated total cross sections, plotted versus the anomalous coupling κ_{tc}, for the process $t\bar{t} \to W^{\pm} bZc \to l^{\pm}\nu, l^{\pm}l^{\mp}jj$, where $l = e, \mu$ and j denotes a jet from a b or c quark. We see that for κ_{tc} in the range of interest, the signal cross section at the Tevatron is rather small, of the order of a few fb, while at LHC energies, it is about two orders of magnitude larger. However, the final state of the events is quite distinct: three isolated charged leptons, two of which reconstruct a Z, large missing transverse energy (E_T^{miss}), and two hard jets coming from the b or c quarks. The only irreducible background to this signal is the electroweak process $p\bar{p}, pp \to W^{\pm}ZX \to l^{\pm}\nu l^{+}l^{-}X$. Since the signal events naturally contain two energetic jets from heavy top-quark decays, typically with a transverse momentum of order $p_T(j) \simeq \frac{1}{2}m_t(1 - M_W^2/m_t^2)$, it is advantageous to demand two observable jets in the events to suppress the WZ background.

To better address the feasibility of observing the effects from κ_{tc}, we need to consider detector effects and to impose some acceptance cuts on the transverse momentum (p_T), pseudo-rapidity (η), and the separation in azimuthal angle-pseudo rapidity plane (ΔR) for the charged leptons and jets. We choose for the Tevatron the acceptance cuts:

$$\begin{aligned} &p_T^l > 15 \text{ GeV}, \quad |\eta^l| < 2.5, \quad \Delta R_{lj} > 0.4, \quad E_T^{miss} > 20 \text{ GeV}, \\ &p_T^j > 15 \text{ GeV}, \qquad |\eta^j| < 2.5, \quad \Delta R_{jj} > 0.4. \end{aligned} \tag{12}$$

For the LHC the equivalent cuts chosen are:

$$\begin{aligned} &p_T^l > 25 \text{ GeV}, \quad |\eta^l| < 3, \quad \Delta R_{lj} > 0.4, \quad E_T^{miss} > 30 \text{ GeV}, \\ &p_T^j > 30 \text{ GeV}, \qquad |\eta^j| < 3, \quad \Delta R_{jj} > 0.4. \end{aligned} \tag{13}$$

With these minimal acceptance cuts, the signal and background rates at the Tevatron and LHC are given in Fig. 3 (dotted curves).

There is an easy way to improve the signal-to-background ratio to some extent. Recall the argument given above that the jet $p_T(j)$ spectrum for the signal peaks around $m_t/2$. In contrast, the QCD jets in the background events are near the threshold region (determined by the cutoff imposed) and extend further, if phase space is available as it is at LHC energies.

This feature is demonstrated in Fig. 4, where the differential cross section versus a scalar sum of the jet's transverse momenta,

$$p_T(jj) \equiv |\vec{p}_T(j_1)| + |\vec{p}_T(j_2)|,$$

is plotted, where the anomalous coupling κ_{tc} has been chosen to be 0.14, for which the signal and the background have about the same total rate. We see indeed, that the $p_T(jj)$ spectrum for the signal peaks near m_t and does not significantly depend on the c.m. energy. If we further impose a cut on $p_T(jj)$,

$$80 \text{ GeV} < p_T(jj) < 250 \text{ GeV}, \tag{14}$$

the background is reduced, but the signal is hardly affected. The effect of this cut is shown in Fig. 3 by the dashed curves.

An important advantage of searching for top-quark flavor-changing decays in the $t \to Zc \to l^+l^-c$ channel is the full reconstructability of the top-quark mass. The mass variable $M(l^+l^-j)$ from the decay $t \to Zc \to l^+l^-j$ should reconstruct m_t, and is clearly the most characteristic quantity for the signal. Similarly, the mass variable $M(l\nu j)$ from the decay $t \to Wb \to l\nu j$ should also peak near m_t. However, in the latter case there is a two-fold ambiguity in constructing the neutrino momentum along the beam direction [23] due to the lack of knowledge of the parton c.m. frame. For an input M_W and massless leptons, using the measured charged lepton momentum (p^ℓ) and the *transverse* momentum of the neutrino (p_T^ν), the two solutions for the *longitudinal* momentum of the neutrino are given by

$$p_L^\nu = \frac{1}{2\,(p_T^\ell)^2}\left\{p_L^\ell\left(M_W^2 + 2\,\mathbf{p}_T^\ell\cdot\mathbf{p}_T^\nu\right) \pm p^\ell\left[\left(M_W^2 + 2\,\mathbf{p}_T^\ell\cdot\mathbf{p}_T^\nu\right)^2 - 4\,(p_T^\ell)^2\,(p_T^\nu)^2\right]^{1/2}\right\}. \tag{15}$$

Although the intrinsic top-quark width is only about 1.5 GeV for $m_t = 175$ GeV, the signal peaks for these mass variables will not be as narrow and sharp, due to the finite detector resolution for measuring the energy of the charged leptons and hadrons. We simulate these detector effects by assuming a Gaussian energy smearing for the electromagnetic and hadronic calorimetry as follows:

$$\Delta E/E = 30\%/\sqrt{E} \oplus 1\%, \quad \text{for leptons}$$
$$= 80\%/\sqrt{E} \oplus 5\%, \quad \text{for jets.} \tag{16}$$

Moreover, in constructing $M(Zc) = M(l^+l^-j)$, because we cannot straightforwardly identify the c-quark jet, we examine both jets in the final state and keep the one of the two mass values which is numerically closer to $m_t = 175$ GeV. Figure 5 shows the differential cross section for the reconstructed mass variable $M(l^+l^-j)$ obtained by this procedure for the signal (solid histogram) and background (dashed histogram) at the Tevatron a) and the LHC b). We see that the signal has a sharp distribution near m_t with a width of about 20 GeV, dominated by the hadronic calorimeter resolution of Eq. (16). In this figure, the anomalous coupling κ_{tc} has been chosen to be 0.1, a value for which the signal and the background have about the same total rate. One can further study the mass variable $M(Wb) = M(l\nu j)$. Here we once again make use of the knowledge of the value of m_t and choose from the two $M(l\nu j)$ values the one which is numerically closer to m_t. Figure 6 presents the differential cross section for the variable $M(l^\pm\nu j)$ for the signal (solid histogram) and background (dashed histogram) for the Tevatron and the LHC. We see again a sharp distribution near m_t with a width now about 30 GeV.

Making use of the distributions of Figs. 5 and 6, which are rather impressive, allows us to estimate the statistical sensitivity with which one can hope to measure κ_{tc}. This can be carried out by searching for events which fall within the ranges

$$|M(l^+l^-j) - m_t| < 20\,\text{GeV}, \quad |M(l^\pm\nu j) - m_t| < 40\,\text{GeV}. \tag{17}$$

The solid curves in Fig. 3 show the signal and background rates with all cuts in Eqs. (12), (13), (14) and (17). Note again that the cuts in Eq. (17) do little to diminish the signal. Figure. 7 gives the sensitivity with which κ_{tc} can be measured as a function of accumulated luminosity in units of fb^{-1} at the Tevatron a) and the LHC b) for a 99% Confidence Level (C.L.) (solid) and a 95% C.L. (dashed). Poisson statistics has been adopted in determining the Confidence Level when the number of events is small. For a large number of events,

a 95% (99%) C.L. in this scheme approximately corresponds to Gaussian statistics with $\sigma \equiv N_S/\sqrt{N_S + N_B} \simeq 3(4)$.

In probing κ_{tc} at a 99% C.L., we find the sensitivity to be, at the Tevatron

$$\begin{aligned}
&\text{with } 1\ \text{fb}^{-1}: && \kappa_{tc} \sim 0.42 && \text{or} \quad BR(t \to Zc) \sim 9\% \\
&\text{with } 3\ \text{fb}^{-1}: && \kappa_{tc} \sim 0.26 && \text{or} \quad BR(t \to Zc) \sim 3\% \\
&\text{with } 10\ \text{fb}^{-1}: && \kappa_{tc} \sim 0.16 && \text{or} \quad BR(t \to Zc) \sim 1\% \\
&\text{with } 30\ \text{fb}^{-1}: && \kappa_{tc} \sim 0.11 && \text{or} \quad BR(t \to Zc) \sim 0.6\%\,,
\end{aligned} \tag{18}$$

and at the LHC

$$\begin{aligned}
&\text{with } 1\ \text{fb}^{-1}: && \kappa_{tc} \sim 9 \cdot 10^{-2} && \text{or} \quad BR(t \to Zc) \sim 4 \cdot 10^{-3} \\
&\text{with } 10\ \text{fb}^{-1}: && \kappa_{tc} \sim 4 \cdot 10^{-2} && \text{or} \quad BR(t \to Zc) \sim 8 \cdot 10^{-4} \\
&\text{with } 100\ \text{fb}^{-1}: && \kappa_{tc} \sim 2 \cdot 10^{-2} && \text{or} \quad BR(t \to Zc) \sim 2 \cdot 10^{-4}\,.
\end{aligned} \tag{19}$$

We see that a high luminosity Tevatron or the LHC would have good potential to explore this anomalous $Z\bar{t}c$ coupling.

IV. DISCUSSIONS AND SUMMARY

We have thus far only concentrated on the leptonic decays $Z \to l^+l^-$. Given the possibility of efficient b-tagging at the Tevatron [1] and LHC [24] detectors, one may consider also studying the decay $Z \to b\bar{b}$, with a branching fraction of about 15%. The signal rate would be approximately doubled and this mode might prove quite interesting if one could keep the QCD background under control with b-tagging.

Although not addressed in this paper, it may be equally possible that there exist other effective operators resulting in flavor-changing neutral current interactions, such as $g\bar{t}c$ and $\gamma\bar{t}c$. These operators may have different physics origin and should be studied separately. In a hadron collider environment, the signals associated with these vertices may not be easily separated from the QCD backgrounds. This issue is currently under investigation [25].

To summarize, we have examined the low energy experimental constraints on a possible

anomalous top-quark coupling associated with the flavor-changing neutral current vertex $Z\bar{t}c$. The limits derived from the current experimental data are

$$\kappa_L \leq 0.05; \quad \kappa_R \leq 0.29. \tag{20}$$

We have studied the experimental observability of the induced rare decay mode $t \to Zc$, both at the Fermilab Tevatron and at the LHC. At a 99% C.L., a three-year running of the Tevatron Main Injector (3 fb^{-1}) would reach a sensitivity of BR($t \to Zc$) $\simeq$3%; with an integrated luminosity of 10 fb^{-1} at an upgraded Tevatron, one should be able to explore new physics at a level of BR($t \to Zc$) $\simeq$1%. At the LHC, one can reach a value of $\kappa_{tc} \simeq 0.02$ or BR($t \to Zc$) $\simeq 2 \cdot 10^{-4}$ with a luminosity of 100 fb^{-1}. Because of the cleanliness of the experimental signature and the smallness of the SM prediction for this channel, observation of this rare decay would clearly signal new physics beyond the SM. If seen, such a signal would provide important clues to understanding the mechanism of electroweak symmetry breaking and possibly fermion (especially top-quark) mass generation.

V. ACKNOWLEDGMENTS

We would like to thank C. Hill, S. Parke, S. Willenbrock for discussions. X.Z. would like to thank the Fermilab theory group for the hospitality during the final stage of this work. This work was supported in part by the U.S. Department of Energy under Contracts DE-FG03-91ER40674 (T.H.), DE-FG03-91ER40662 (R.D.P.), DE-FG02-94ER40817 (X.Z.).

APPENDIX: HELICITY AMPLITUDES FOR TOP TO Z-CHARM

In the limit of $m_c = 0$, the non-zero helicity amplitudes for $t \to cZ$ decay, denoted by $\mathcal{M}(\lambda_t, \lambda_c, \lambda_Z)$, after suppressing a common factor $[g/(2\cos\theta_W)]\sqrt{2m_t E_c}$, are

$$\mathcal{M}(--0) = \frac{m_t}{M_Z}\kappa_L \cos\frac{\theta}{2},$$
$$\mathcal{M}(---) = \sqrt{2}\,\kappa_L \sin\frac{\theta}{2},$$

$$
\begin{aligned}
\mathcal{M}(-+0) &= \frac{m_t}{M_Z}\kappa_R \sin\frac{\theta}{2}e^{-i\phi}, \\
\mathcal{M}(-++) &= \sqrt{2}\,\kappa_R \cos\frac{\theta}{2}e^{-i\phi}, \\
\mathcal{M}(+-0) &= -\frac{m_t}{M_Z}\kappa_L \sin\frac{\theta}{2}e^{i\phi}, \\
\mathcal{M}(+--) &= \sqrt{2}\kappa_L \cos\frac{\theta}{2}e^{i\phi}, \\
\mathcal{M}(++0) &= \frac{m_t}{M_Z}\kappa_R \cos\frac{\theta}{2}, \\
\mathcal{M}(+++) &= -\sqrt{2}\,\kappa_R \sin\frac{\theta}{2}.
\end{aligned} \tag{21}
$$

Here θ is the polar angle of the c quark in the top-quark rest frame, measured with respect to the top-quark momentum direction; similarly, the helicities (λ's) have been defined in the top-quark rest frame and with respect to the moving particle direction.

REFERENCES

[1] F. Abe, et al. (CDF Collaboration), Phys. Rev. Lett. **74**, 2626 (1995); S. Abachi et al. (D0 Collaboration), Phys. Rev. Lett. **74**, 2632 (1995).

[2] For a recent review, see, *e. g.*, H. Neuberger, in *Proceedings of the XXVI International Conference on High Energy Physics*, Dallas, Texas, 1992, edited by J. Sanford, AIP Conf. Proc. No. 272 (AIP, New York, 1992), Vol. II, p. 1360.

[3] G. 't Hooft, in *Recent Developments in Gauge Theories*, Proceedings of the Cargese Summer Institute, Cargese, France, 1979, edited by G. 't Hooft et al., NATO Advanced Study Institute Series B; Physics Vol. 59 (Plenum, New York, 1980).

[4] R. D. Peccei and X. Zhang, Nucl. Phys. **B337**, 269 (1990).

[5] See, *e. g.*, D. O. Carlson, E. Malkawi and C.-P. Yuan, Phys. Lett. **B337**, 145 (1994); and references therein.

[6] See, *e. g.*, D. Atwood, A. Kagan and T. Rizzo, SLAC-PUB-6580 (hep-ph/9407408); and references therein.

[7] R. Batley, talk presented at DPF'94, Albuquerque, New Mexico, 1994.

[8] For an early discussion, see, R. D. Peccei, S. Peris and X. Zhang, Nucl. Phys. **B349**, 305 (1991).

[9] For an early discussion, see, H. Fritzsch, Phys. Lett. **B224**, 423 (1989).

[10] C.T. Hill, Phys. Lett. **B266**, 419 (1991); Phys. Lett. **B345**, 483 (1995); B. Holdom, Phys. Lett. **B339**, 114 (1994); Phys. Lett. **B351**, 279 (1995).

[11] B. Grzadkowski, J.F. Gunion and P. Krawczyk, Phys. Lett. B268, 106 (1991); G. Eilam, J.L. Hewett and A. Soni, Phys. Rev. D44, 1473 (1991); M. Luke and M. J. Savage, Phys. Lett. **B307**, 387 (1993); G. Couture, C. Hamzaoui and H. König, UQAM-PHE-94/08, Sept. 1994 (hep-ph/9410230).

[12] T. P. Cheng and M. Sher, Phys. Rev. **D35**, 3484 (1987); W. S. Hou, Phys. Lett. **B296**, 179 (1992); L. J. Hall and S. Weinberg, Phys. Rev. **D48**, R979 (1993); D. Atwood, L. Reina, A. Soni, SLAC-PUB-95-6927 (hep-ph/9506243).

[13] W. Buchmüller and M. Gronau, Phys. Lett. **B220**, 641 (1989).

[14] Particle Data Group, *Review of Particle Properties*, Phys. Rev. D50, 1173 (1994).

[15] C.P. Burgess et al., Phys. Rev. **D49**, 6115 (1994); E.W.J. Glover and J.J. van der Bij, in *Z-physics at LEP I*, CERN yellow report CERN 89-08, Vol. 2, P.42, ed. G. Altarelli, R. Kleiss and C. Verzegnassi.

[16] R. K. Ellis, Phys. Lett. **B259**, 492 (1991); E. Laenen, J. Smith and W. L. van Neerven, Phys. Lett. **B321**, 254 (1994).

[17] S. Willenbrock and D. Dicus, Phys. Rev. **D34**, 155 (1986); C.-P. Yuan, Phys. Rev. **D41**, 42 (1990); R. K. Ellis and S. Parke, Phys. Rev. **D46**, 3785 (1992); D. Carlson and C.-P. Yuan, Phys. Lett. **B306**, 386 (1993); G. Bordes and B. van Eijk, Nucl. Phys. **B435**, 23 (1995).

[18] S. Cortese and R. Petronzio, Phys. Lett. **B253**, 494 (1991); T. Stelzer and S. Willenbrock, DTP/95/40 (hep-ph/9505433).

[19] A. D. Martin, R. G. Roberts and W. J. Stirling, Phys. Rev. **D50**, 6734 (1994).

[20] F. Berends, J. B. Tausk, and W. T. Giele, Phys. Rev. **D47**, 2746 (1993).

[21] V. Barger, E. Mirkes, R. J. N. Phillips, and T. Stelzer, Phys. Lett. **B338**, 336 (1994).

[22] V. Barger, J. Ohnemus and R. Phillips, Int. J. Mod. Phys. **A**, 617 (1989).

[23] J. Stroughair and C. Bilchak, Z. Phys. **C 26**, 415 (1984); J. Gunion, Z. Kunszt, and M. Soldate, Phys. Lett. **B 163**, 389 (1985); J. Gunion and M. Soldate, Phys. Rev. **D 34**, 826 (1986); W. J. Stirling *et al.*, Phys. Lett. **B 163**, 261 (1985); J. Cortes, K. Hagiwara, and F. Herzog, Nucl. Phys. **B 278**, 26 (1986).

[24] CMS Collaboration, Technical Proposal, CERN/LHCC/94-38; ATLAS Collaboration, Technical Proposal, CERN/LHCC/94-43.

[25] T. Han, L. Li, K. Whisnant, B.-L. Young and X. Zhang (in preparation).

FIGURES

FIG. 1. Branching fraction $\Gamma(t \to Zc)/\Gamma(t \to Wb)$ plotted versus the anomalous coupling κ_{tc} for m_t =160 and 200 GeV.

FIG. 2. Total cross section for $p\bar{p}, pp \to t\bar{t}X \to W^{\pm}bZcX \to l^{\pm}\nu l^{+}l^{-}X$ in units of fb for m_t = 175 GeV, at the Tevatron and LHC plotted versus κ_{tc}. The arrows on the right-hand scale indicate the inclusive rates at the Tevatron (lower arrow) and LHC (upper arrow) for $p\bar{p}, pp \to W^{\pm}ZX \to l^{\pm}\nu l^{+}l^{-}X$ production.

FIG. 3. Expected number of events for m_t = 175 GeV at the Tevatron with an integrated luminosity of 10 fb^{-1} and the LHC with 100 fb^{-1} plotted versus κ_{tc}. The horizontal lines are for the $W^{\pm}Zjj$ background. The dotted curves are the rates after imposing the minimal acceptance cuts in Eqs. (12) and (13); the dashed curves also include the cuts in Eq. (14); the solid curves include, in addition, the mass cuts in Eq. (17). A Gaussian energy smearing according to Eq. (16) is included in the simulation.

FIG. 4. Differential cross sections $d\sigma/dp_T(jj)$ in units of fb/GeV at a). the Tevatron and b). the LHC with m_t = 175 GeV and κ_{tc} = 0.14 for the signal (solid histogram) and background (dashed histogram). The minimal acceptance cuts in Eqs. (12) and (13) have been imposed.

FIG. 5. Differential cross sections $d\sigma/dM(l^{+}l^{-}j)$ in units of fb/GeV at a). the Tevatron and b). the LHC with m_t = 175 GeV and κ_{tc} = 0.1 for the signal (solid histogram) and background (dashed histogram). The acceptance cuts in Eqs. (12), (13) and (14) have been imposed.

FIG. 6. Same as Fig. 5, but for the reconstructed mass distributions $d\sigma/dM(l^{\pm}\nu j)$.

FIG. 7. Sensitivity on κ_{tc} for m_t = 175 GeV plotted versus the accumulated luminosity (fb^{-1}) at a). the Tevatron and b). the LHC for a 99% C.L. (solid) and a 95% C.L. (dashed).

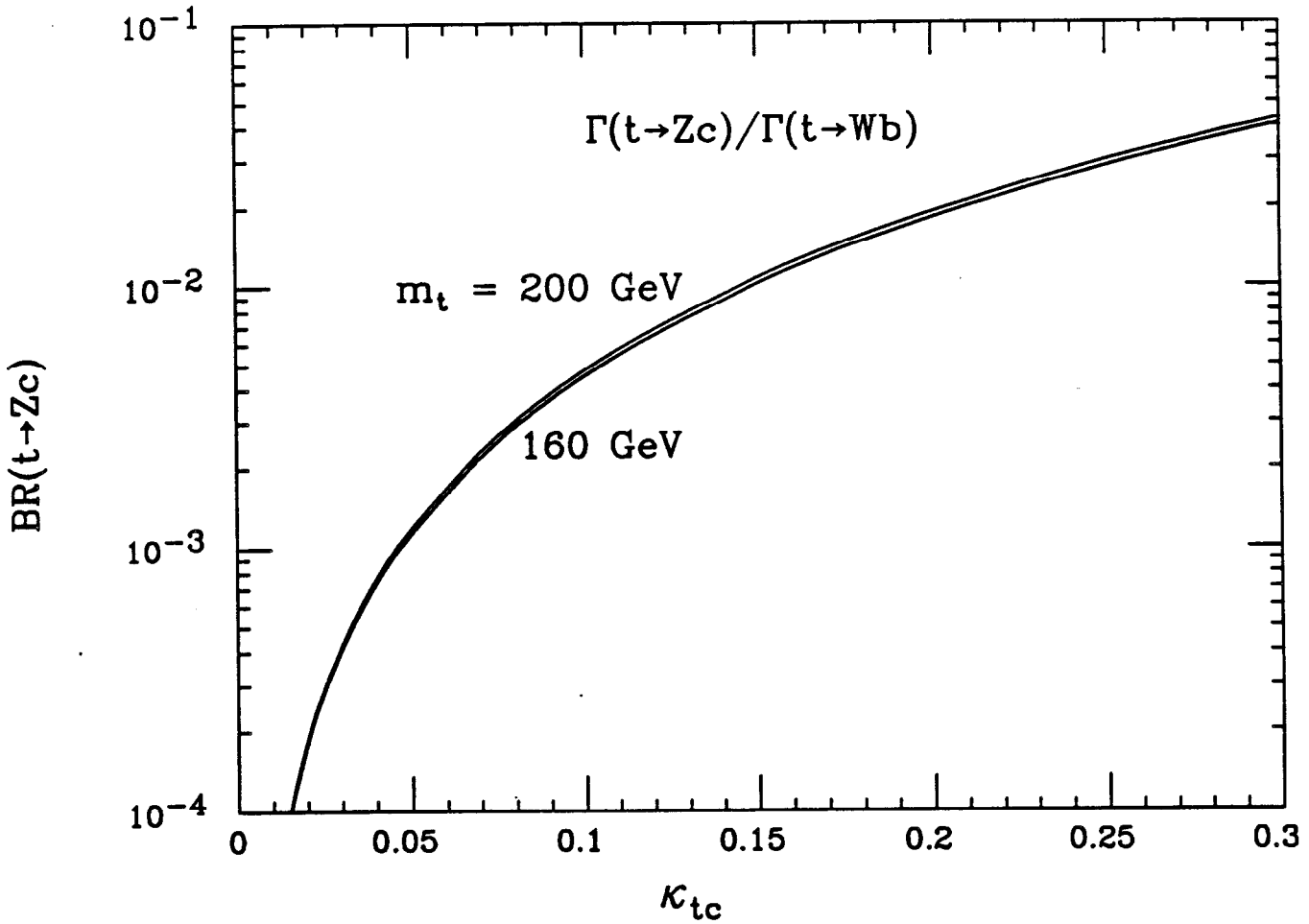
10^{-1}
10^{-2}
10^{-3}
10^{-4}
BR(t→Zc)
Γ(t→Zc)/Γ(t→Wb)
m_t = 200 GeV
160 GeV
0
0.05
0.1
0.15
0.2
0.25
0.3
κ_{tc}

Figure 1

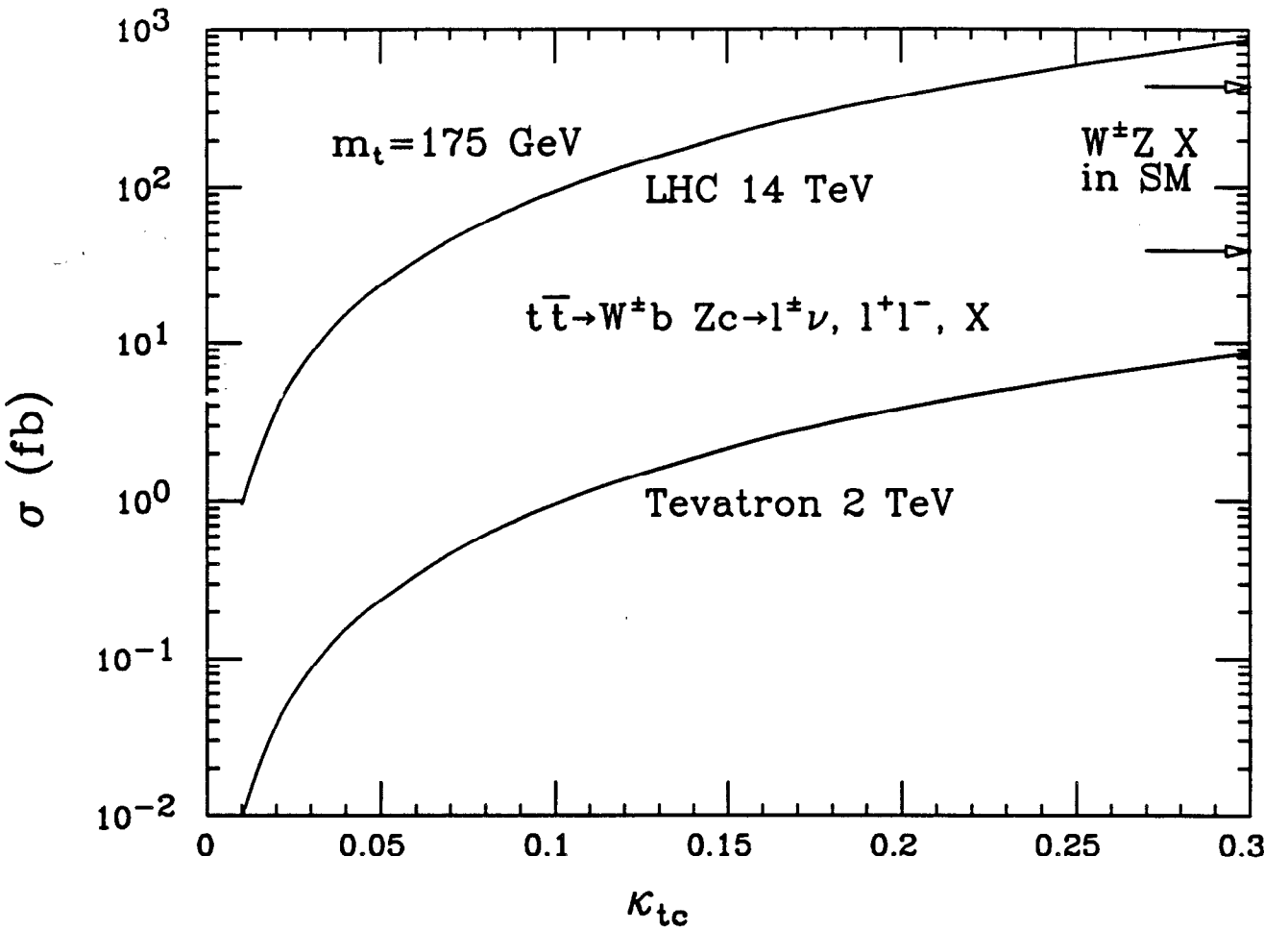
10^3
10^2
10^1
10^0
10^{-1}
10^{-2}
σ (fb)
m_t=175 GeV
LHC 14 TeV
$W^{\pm}Z$ X
in SM
$t\bar{t} \to W^{\pm}b\ Zc \to l^{\pm}\nu,\ l^+l^-,\ X$
Tevatron 2 TeV
0
0.05
0.1
0.15
0.2
0.25
0.3
κ_{tc}

Figure 2

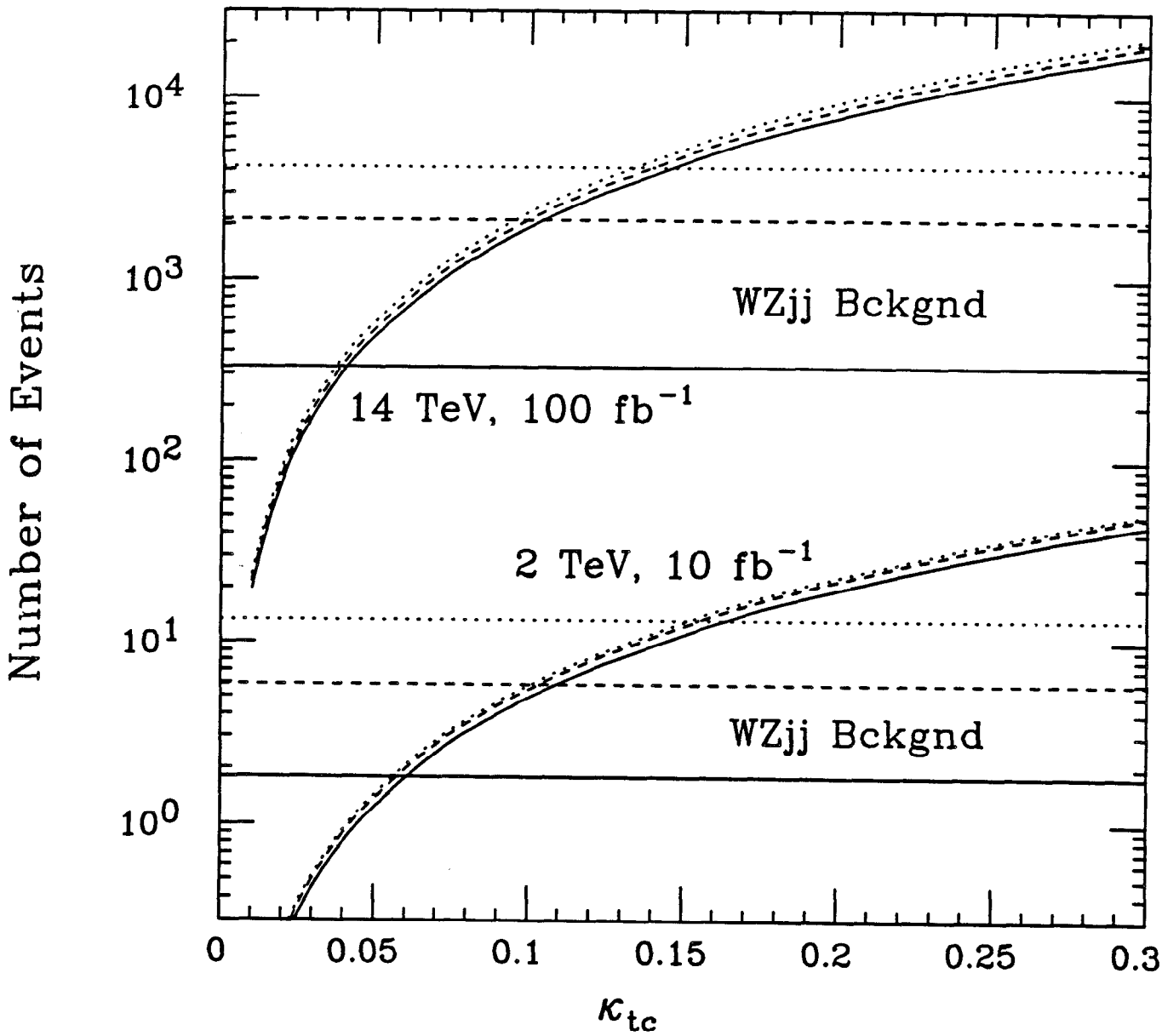
Number of Events
10^4
10^3
10^2
10^1
10^0
WZjj Bckgnd
14 TeV, 100 fb^{-1}
2 TeV, 10 fb^{-1}
WZjj Bckgnd
0
0.05
0.1
0.15
0.2
0.25
0.3
κ_{tc}

Figure 3

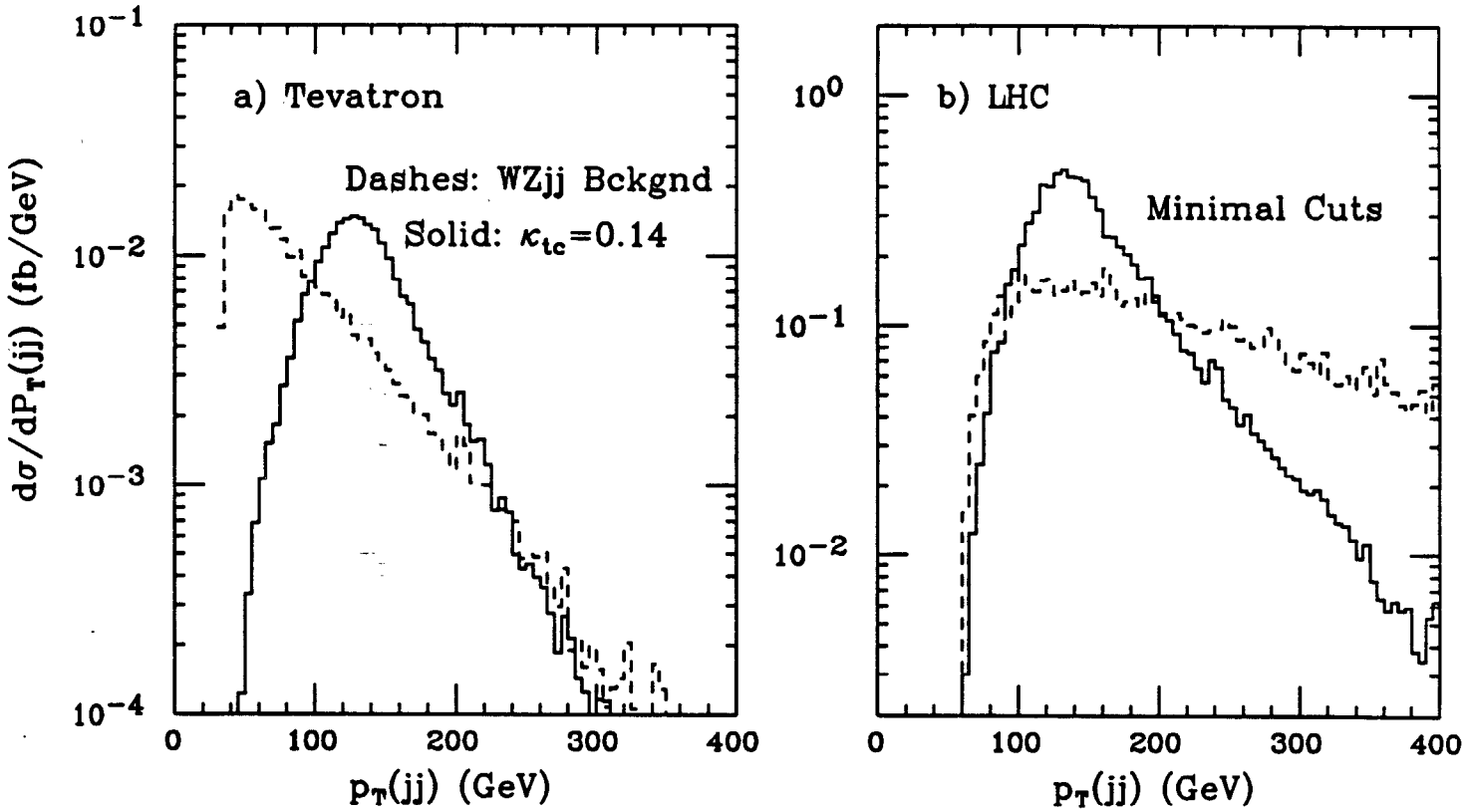
a) Tevatron
Dashes: WZjj Bckgnd
Solid: κ_{tc}=0.14
$d\sigma/dP_T(jj)$ (fb/GeV)
$p_T(jj)$ (GeV)
b) LHC
Minimal Cuts
$p_T(jj)$ (GeV)

Figure 4

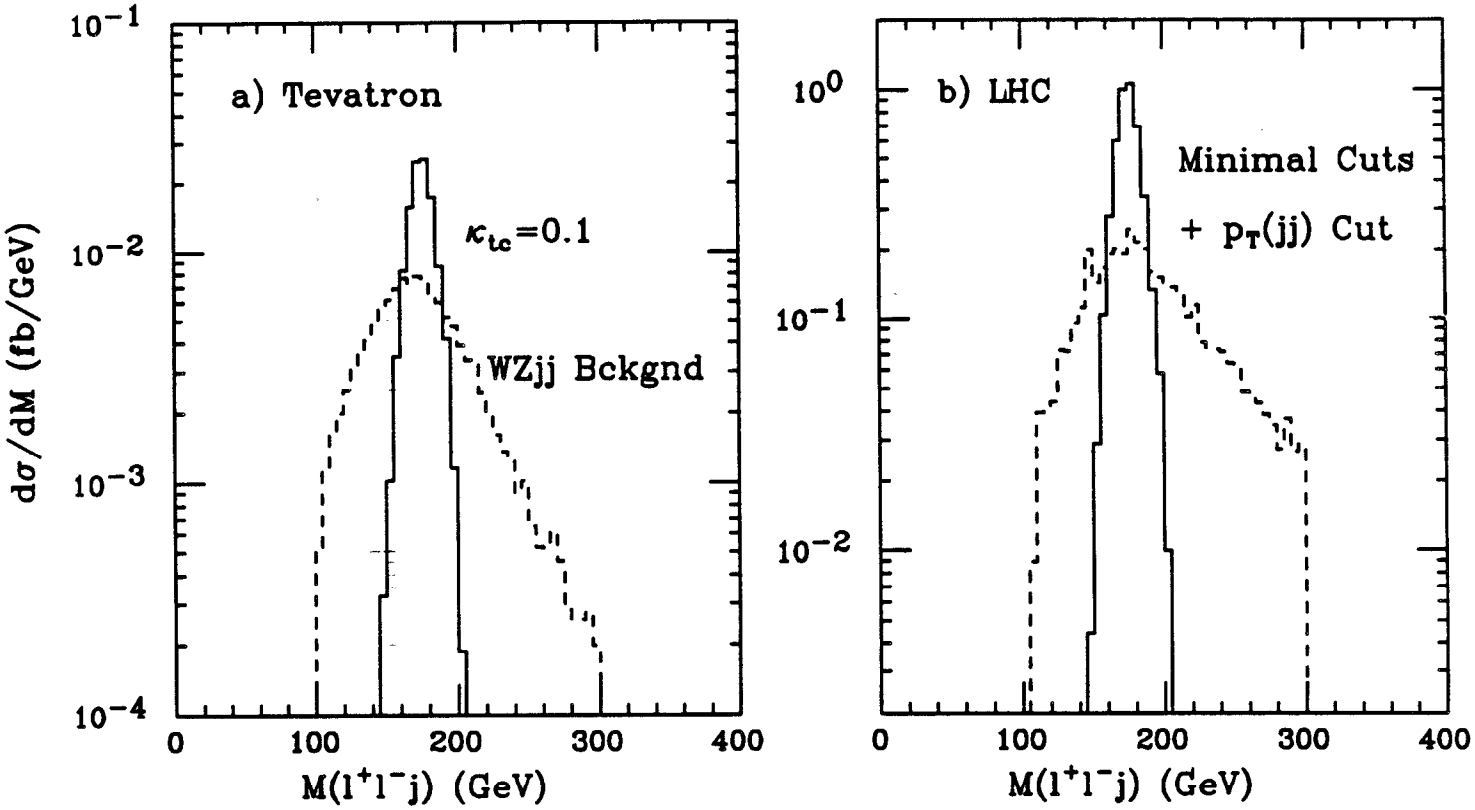
a) Tevatron
κ_{tc}=0.1
WZjj Bckgnd
$d\sigma/dM$ (fb/GeV)
10^{-1}
10^{-2}
10^{-3}
10^{-4}
0
100
200
300
400
$M(l^+l^-j)$ (GeV)
b) LHC
Minimal Cuts
+ $p_T(jj)$ Cut
10^0
10^{-1}
10^{-2}
0
100
200
300
400
$M(l^+l^-j)$ (GeV)

Figure 5

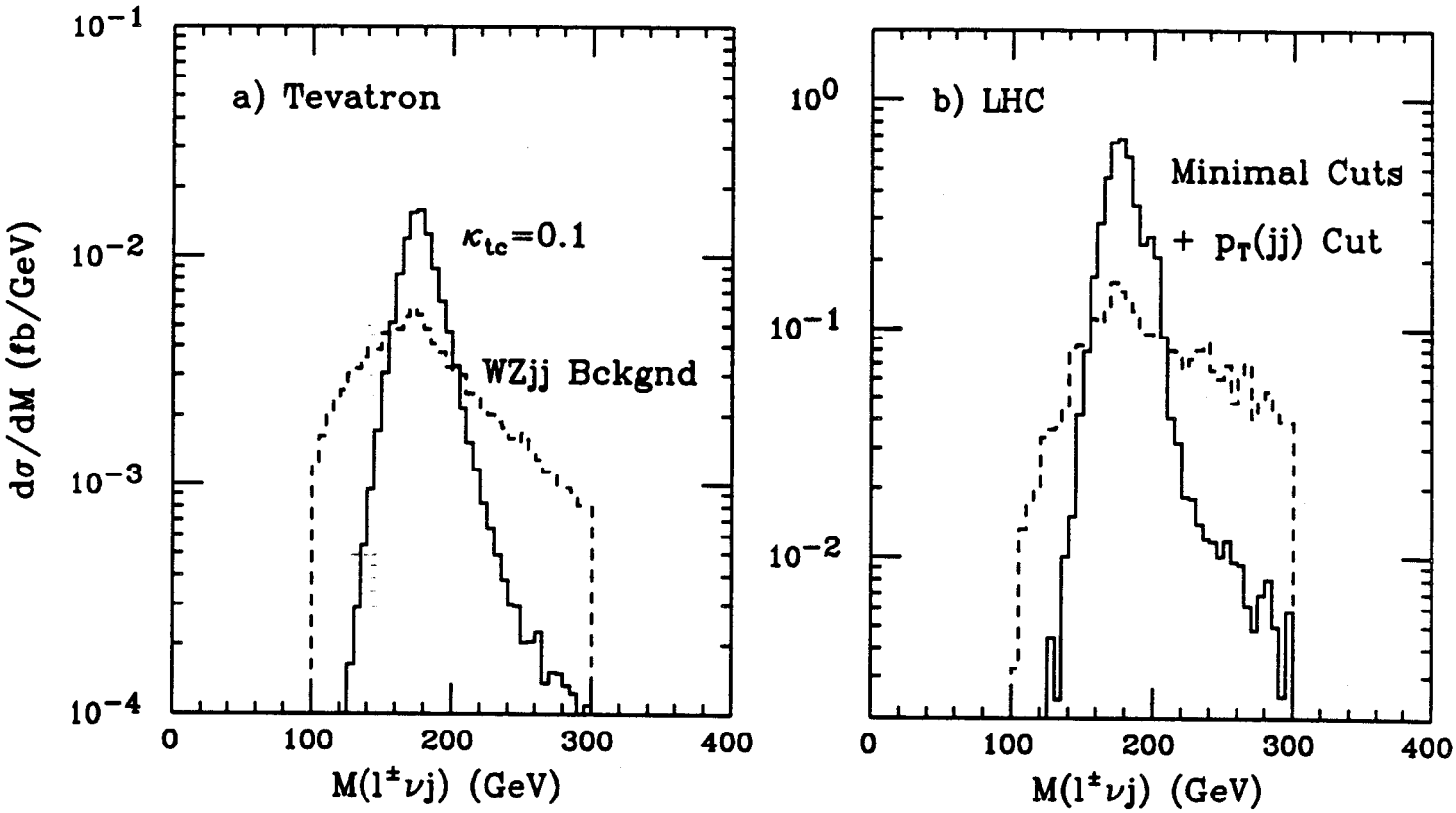
a) Tevatron
κ_{tc}=0.1
WZjj Bckgnd
$d\sigma/dM$ (fb/GeV)
$M(l^{\pm}\nu j)$ (GeV)
b) LHC
Minimal Cuts
+ $p_T(jj)$ Cut
$M(l^{\pm}\nu j)$ (GeV)

Figure 6

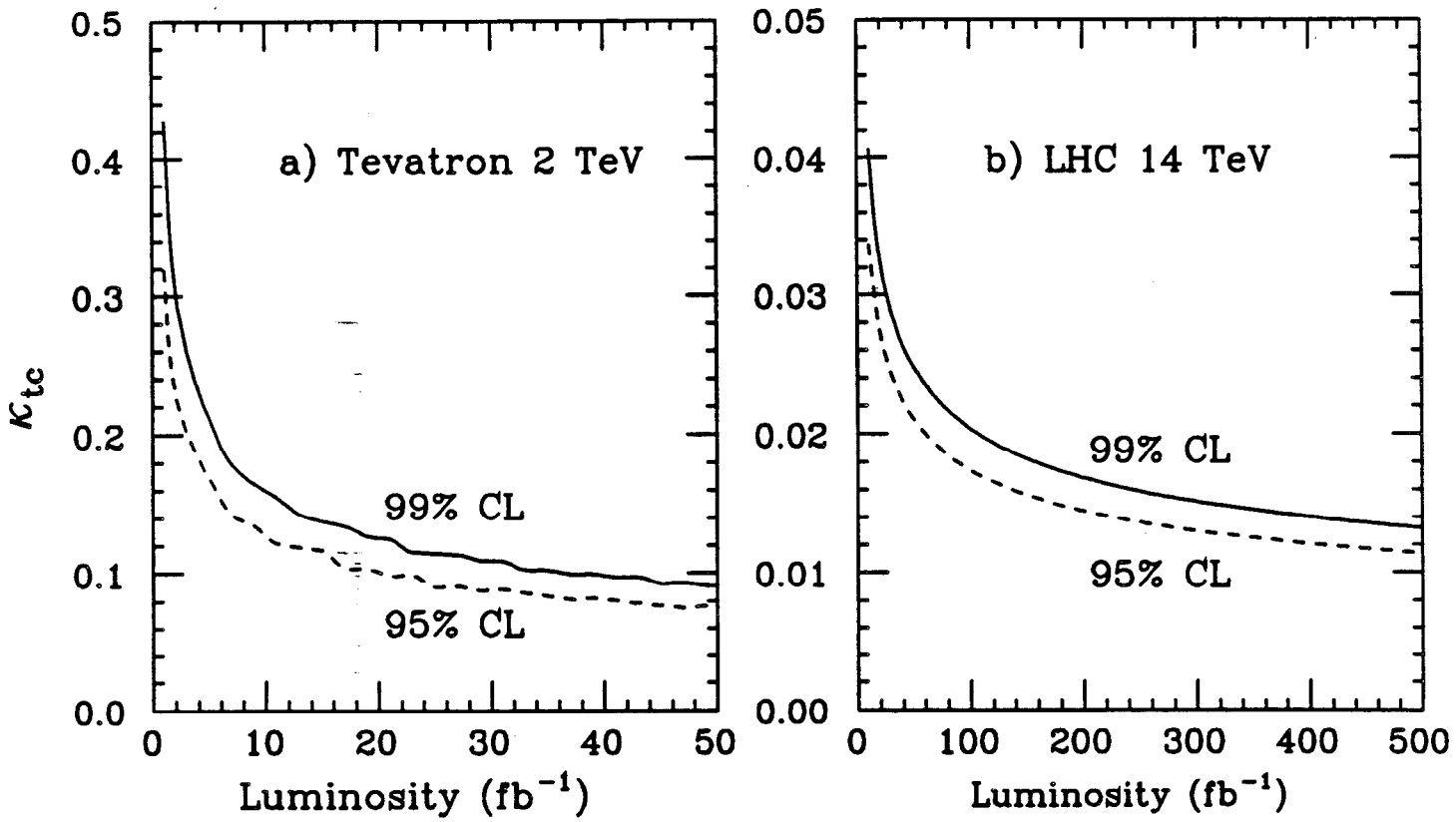
0.5
0.4
0.3
0.2
0.1
0.0
κ_{tc}
a) Tevatron 2 TeV
99% CL
95% CL
0
10
20
30
40
50
Luminosity (fb^{-1})
0.05
0.04
0.03
0.02
0.01
0.00
b) LHC 14 TeV
99% CL
95% CL
0
100
200
300
400
500
Luminosity (fb^{-1})

Figure 7